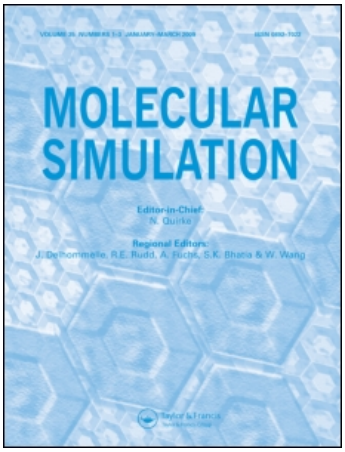

Molecular Simulation
Publication details, including instructions for authors and subscription information:
http://www.informaworld.com/smpp/title~content=t713644482

The effect of cooperativity on hydrogen bonding interactions in native cellulose Iβ from *ab initio* molecular dynamics simulations

Xianghong Qian[a]
[a] Department of Mechanical Engineering and School of Biomedical Engineering, Colorado State University, Fort Collins, USA

To cite this Article Qian, Xianghong(2008) 'The effect of cooperativity on hydrogen bonding interactions in native cellulose Iβ from *ab initio* molecular dynamics simulations', Molecular Simulation, 34: 2, 183 — 191
To link to this Article: DOI: 10.1080/08927020801961476
URL: http://dx.doi.org/10.1080/08927020801961476

Molecular Simulation
Vol. 34, No. 2, February 2008, 183–191

Taylor & Francis
Taylor & Francis Group

The effect of cooperativity on hydrogen bonding interactions in native cellulose Iβ from *ab initio* molecular dynamics simulations

Xianghong Qian*

Department of Mechanical Engineering and School of Biomedical Engineering, Colorado State University, Fort Collins, USA

(Received 12 December 2007; final version received 2 February 2008)

Hydrogen bonding cooperativity plays an important role in the stability of α-helices, β-sheets and many other hydrogen bonding systems. Here *ab initio* calculations were performed to determine the cooperative effect on hydrogen bonding structures in native crystalline cellulose Iβ. Both isolated and paired cellulose chains with degree of polymerisation varying from 2 to 7 were investigated. A highly cooperative hydrogen bonding interaction was found in the paired cellulose chains, particularly between the inter-chain and intra-chain hydrogen bonds. An enhancement in hydrogen bonding strength was also observed when infinite cellulose chains were paired to form cellulose sheets, and when cellulose sheets were stacked to form three dimensional cellulose crystalline structures. This hydrogen bonding cooperativity is likely due to the electron delocalisation effect.

Keywords: cooperativity; hydrogen bonding; cellulose; *ab initio* calculations

1. Introduction

Biomass consists mainly of cellulose, hemicellulose and lignin. Cellulose is a linear glucose polymer connected via glycosidic β-1,4 linkage. It is the most abundant biopolymer on earth. Cellulose elementary fibril in higher plants is believed to consist of only 36 cellulose chains with about 3–5 nanometers in diameter [1, 2]. These cellulose fibrils are surrounded by hemicelluloses forming the so-called microfibrils [3]. Cellulose exhibits various degrees of crystallinity ranging from amorphous, sub-crystalline to crystalline [2]. The inner chains of the elementary fibrils are thought to be the only true crystalline cellulose. Due to the interaction with the surrounding hemicelluloses, cellulose structure becomes more disordered when the chains are closer to the cellulose-hemicellulose interface. So far, native celluloses can only be synthesised in nature by cellulose synthase [3,4]. It was proposed that there are two types of native crystalline celluloses, cellulose Iα and Iβ, and they co-exist in different organisms with different proportions [5]. The crystalline structures and the hydrogen bonding networks in cellulose Iα and Iβ were elucidated recently using x-ray and neutron diffraction techniques [6,7]. Cellulose Iα has a triclinic crystal structure ($a = 6.717$ Å, $b = 5.9962$ Å, $c = 10.4$ Å, $\alpha = 118.08°$, $\beta = 114.80°$, and $\gamma = 80.37°$) with only one cellobiose unit in each unit cell [6], whereas cellulose Iβ is monoclinic ($a = 7.784$ Å, $b = 8.201$ Å, $c = 10.380$ Å, $\alpha = \beta = 90°$, $\gamma = 96.5°$) with two cellobiose units in each unit cell [7]. One is called the origin chain, whereas the other is called the centre chain. Cellulose Iβ is the major crystal allomorph in higher plants. Our earlier theoretical investigation of the atomic and hydrogen bonding structures in cellulose Iβ using Car-Parrinello based *ab initio* molecular dynamics simulations (CPMD) yielded very good agreement with the experimental results [8].

The native crystalline celluloses are very resistant to chemical and enzymatic acid hydrolysis to break down the polymeric cellulose to monomer glucose [2]. This is thought mainly due to the strong hydrogen bonding interactions in crystalline cellulose Iβ. There are three types of strong hydrogen bonds in crystalline cellulose Iβ as shown in Figure 1 [7]. The O3H on one glucose residue forms an intra-chain hydrogen bond with the ring O5 in the neighbouring residue (O3H···O5). The O2H from the neighbouring residue forms another intra-chain hydrogen bond with the O from O6H group (O2H···O6) of the first residue. Besides these two intra-chain hydrogen bonding interactions, there is the O6H···O3 inter-chain hydrogen bonding interaction between the two neighbouring chains. The O3H and O6H groups are both proton donors and acceptors in the hydrogen bonding interactions. Besides these three hydrogen bonds within the same cellulose sheet, there is also the

*Email: xhqian@engr.colostate.edu

ISSN 0892-7022 print/ISSN 1029-0435 online

DOI: 10.1080/08927020801961476
http://www.informaworld.com

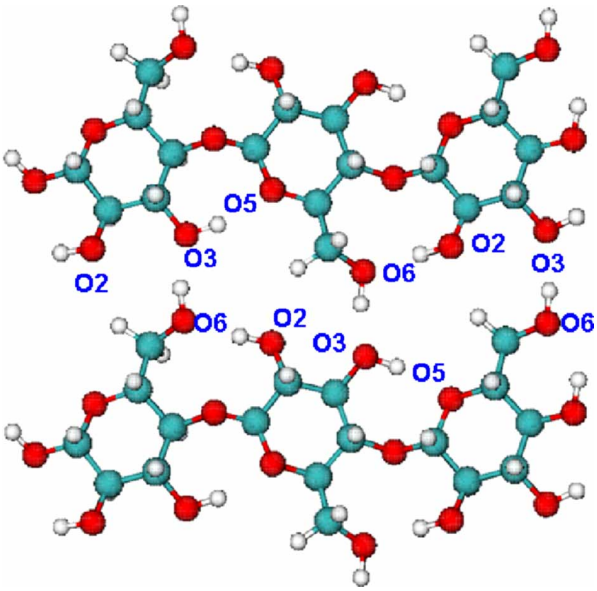

Figure 1. Exhibits both the intra-chain and inter-chain hydrogen bonding network in native cellulose Iβ.

weak C-H···O hydrogen bonding interactions between the neighbouring sheets in cellulose Iβ. Previously we determined the inter-chain binding energy and found that the inter-chain hydrogen bonding interaction is unusually strong with about 7 kcal/mol for each hydrogen bond [8]. Here we investigate the effect of cooperativity on O-H···O hydrogen bonding interaction in cellulose Iβ using *ab initio* molecular dynamics simulations.

Cooperative hydrogen bonding interaction has been discovered to exist in many biological systems including DNA [9], α- and 3_{10}-helices [10–13], β-sheets [14–16], and many other clusters of molecules [17–23] forming hydrogen bonds. Cooperativity refers to the effect of enhanced hydrogen bonding interaction strength due to the presence of neighbouring hydrogen bonds. An increase in bond strength of 60–70% was found for an infinite array of hydrogen bonded formamide molecules [24]. An enhancement of 38–42% was discovered for finite clusters of *N*-methylformamide and *N*-methylacetamide [25,26]. For an infinite α-helical peptide chain, the cooperativity effect enhances each individual bond by more than a factor of two [10]. Cooperativity plays an important role in protein folding and in the stability of α-helices [17]. Cooperative effect was also found to stabilise the β-sheets, which is particularly important for investigating the β-amyloid fibril formation underlying several neurological diseases [14]. Cooperative hydrogen bonding effects were found to be the key determinants of protein backbone amide proton chemical shifts [20]. Besides proteins and DNA, cooperative effect was also found for hydrated mannose, galactose, glucose and lactose and other sugar molecules indicating the role of structural water molecules in the binding of carbohydrates to proteins.

Here, the effect of cooperativity on hydrogen bonding interactions in cellulose Iβ was investigated by determining the hydrogen bond lengths and angles, and its energetics for both the isolated and paired chains with different degrees of polymerisation (DP). Further, several hydrogen bonding structures were determined and compared including an isolated infinite chain, a cellulose sheet formed by pairing the infinite chains, and the cellulose Iβ three dimensional structures formed by stacking the cellulose sheets.

2. Computational method and details

CPMD simulation package [27] was used in the investigation of cooperative hydrogen bonding interactions in the native cellulose Iβ. Our earlier results show that the calculated hydrogen bond lengths and angles in cellulose Iβ using CPMD [8] agree well with the experimental data obtained from x-ray and neutron diffractions [7]. CPMD combines density functional theory with molecular dynamics simulations and is capable of simulating systems up to several thousands of atoms [28]. Contrary to force-field based molecular dynamics simulation methods, CPMD inter-atomic potentials are determined quantum mechanically. It is based on Born–Oppenheimer approximation, which separates the electronic motion from the nuclear motion. The core electrons are frozen whereas the valence electrons are treated using pseudo-potential methods. An extended Largarigen based on Car-Parrinello approach [29] was implemented in CPMD so that both nuclei and electrons follow their respective trajectories. This approach avoids calculating the electron structures from scratch thus speeding up the simulation tremendously.

The valence electrons and semi-core electrons are treated using the density functional developed by Becke [30] and Lee, Yang and Parr [31], BLYP, and are assumed to exist in a psuedopotential exerted by the nuclei and the core electrons. The BLYP function was shown to be appropriate to describe the liquid water [32] and biomolecules [33]. The pseudopotentials used are Troullier-Martin norm-conserving pseudopotential [34]. Plane waves are used as the basic functions in these calculations. Simulations were conducted using a time step of 0.125 femtoseconds. The plane-wave basis set cut-off is 70 Ry, which was shown to be sufficient for bio-molecular simulations in aqueous solution [28]. Three-dimensional periodic boundary conditions are applied. Earlier studies [35] show that density functional theory with BLYP functional yields comparable results to MP2 calculations in predicting hydrogen bonding structures and energies.

In order to determine the effect of cooperativity on hydrogen bonding interactions in cellulose Iβ, the

structures and energetics of cellulose chains with different DP varying from 1–7 were investigated. Since cellulose chains form inter-chain hydrogen bonds as well, the structures and energetics of both the single isolated cellulose chains and paired cellulose chains were determined. The starting structures of the monomer glucose and the cellulose chains with DP varying from 2 to 7 used were taken directly from the crystalline cellulose structures determined from our earlier calculations [8]. For an isolated cellulose chain, each dimension of the simulation box is about 5 Å larger than the dimension of the cellulose chain to avoid interactions between the cellulose chains in the neighbouring unit cells. For paired cellulose chains, the dimension of the unit cell perpendicular to the chains is 8.2 Å, the same as in the native crystalline celluloses so that there will be appropriate hydrogen bonding interactions (O6H···O3) between the chains. By applying periodic boundary condition, the chains in the later case are translated into a two-dimensional cellulose sheets. Except for the dimensions of the unit cells, all other simulation conditions are the same for the isolated and paired cellulose chains in order to minimise the uncertainties in these calculations. Each system was first annealed at 300K for about 1 picosecond (ps) in order to release the strain exerted on the system. It was subsequently quenched to 0 K with the same symmetry. The force on each atom was then minimised to reach the equilibrium structure. The energy and force convergence criteria of 1.0×10^{-5} Ha and 1.0×10^{-5} N/m were used.

Besides varying the DP values, the cellulose hydrogen bonding networks were also investigated by comparing the bond lengths and angles of one isolated chain of infinite length by applying periodic boundary condition in the chain direction, an infinite two dimensional cellulose sheet formed by pairing the chains with the appropriate inter-chain unit cell distance of 8.2 Å, and the three dimensional cellulose structure by stacking the sheets according to the structure of cellulose Iβ. The same procedure and convergence criteria as described earlier were applied.

Suppose the total energy of an isolated optimised glucose molecule is E_1 and the total energy of the optimised isolated chain with n residues is E_n. Also the total energy of each paired cellulose chain with n glucose residues is E_n'. Let $\Delta E_0 = E_2 - E_1$ represents the 0^{th} energy change by adding one glucose residue to the chain. The cooperative hydrogen bonding energy for an isolated cellobiose is defined as $\Delta\Delta E_0 = 0$. Therefore the cooperative hydrogen bond energy for an isolated cellotriose molecule is $\Delta\Delta E_1 = (E_3 - E_2) - \Delta E_0 = E_3 - 2E_2 + E_1$. The cumulative cooperative hydrogen bonding energy for an isolated cellulose chain with n + 2 residues is

$$\triangle\triangle E_n = (E_{n+2} - E_{n+1}) - \triangle E_0 + \triangle\triangle E_{n-1} \quad (n = 1 \text{ to } 5). \tag{1}$$

Likewise, the cumulative cooperative hydrogen bonding energy for the paired cellulose chain with $n + 2$ residues is

$$\triangle\triangle E_n' = (E_{n+2}' - E_{n+1}') - \triangle E_0 - (E_1' - E_1) + \triangle\triangle E_{n-1}' \quad (n = 1 \text{ to } 5) \tag{2}$$

where $E_1' - E_1$ is the energy of the inter-chain O6H···O3 hydrogen bond for paired glucose molecules and $\Delta\Delta E_0' = 0$. The energy difference between the paired chain and isolated chain mainly comes from the formation of inter-chain hydrogen bonds O6H···O3 and also from the contribution of hydrogen bonding cooperative effect as a result of chain alignment.

3. Results and discussion

3.1 The hydrogen bonding structures of the isolated and paired cellulose chains

Figure 2 shows the optimised atomic structures of an isolated glucose molecule and the aligned glucose molecules which form an inter-molecular O6H···O3 hydrogen bond. The inter-chain hydrogen bond length is 2.91 Å, longer than the average O-H···O hydrogen bond length of about 2.76 Å in cellulose Iβ. Figure 3 compares the intra-chain hydrogen bond lengths for a single cellobiose molecule and the paired cellobiose chains. Besides the inter-chain O6H···O3 hydrogen bond, cellobiose possesses two intra-chain O3H···O5 and O2H···O6 hydrogen bonds. The bond lengths and angles

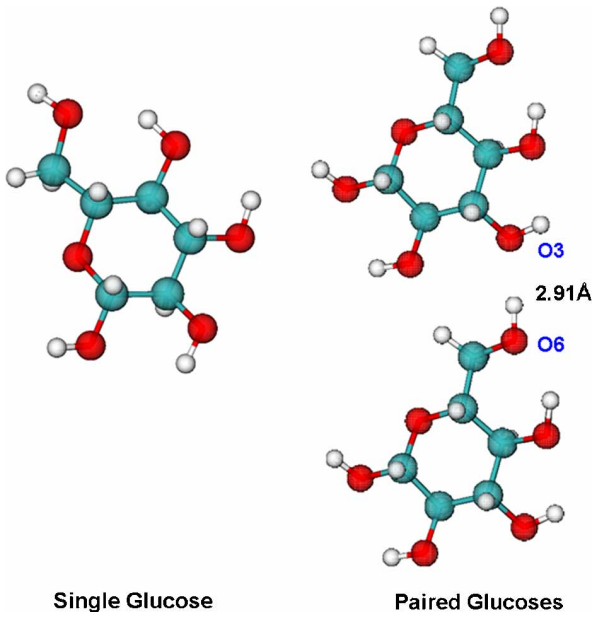

Figure 2. Shows the isolated glucose molecule and paired glucose molecules with one inter-molecular hydrogen bond.

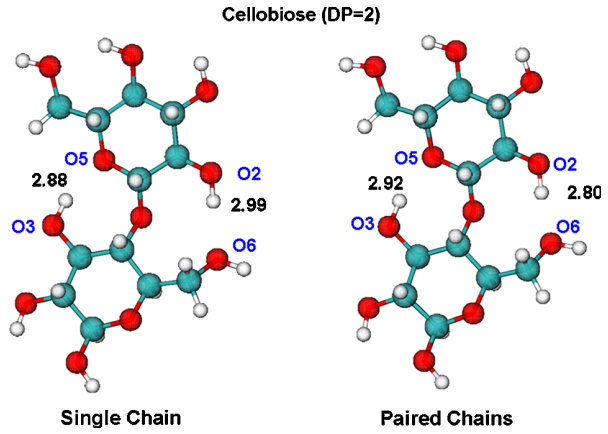

Figure 3. Shows the intra-chain hydrogen bond lengths in an isolated cellobiose molecule and the paired cellobiose molecule.

for O3H···O5 are 2.88 Å, 159.78° and 2.92 Å, 163.07° in the isolated and paired cellobiose chains, respectively. For the O2H···O6 bond, the corresponding bond lengths and angles are 2.99 Å, 168.96° and 2.80 Å, 174.06° respectively. Even though the O3H···O5 bond seems slightly weaker in the paired cellobiose chains, the average hydrogen bond length decreases from 2.935 Å to 2.86 Å before and after pairing indicating an enhancement in the overall hydrogen bonding interaction energy upon chain alignment to form the inter-chain O6H···O3 hydrogen bonds. The average bond angle also increases from 164.3° to 167.1°. This clearly demonstrates the cooperative hydrogen bonding effect between the intra-chain and inter-chain hydrogen bonds in native celluloses.

Figure 4 shows the intra-chain hydrogen bonding network for the isolated cellotriose and paired cellotriose chains. As calculated from the data shown, the average

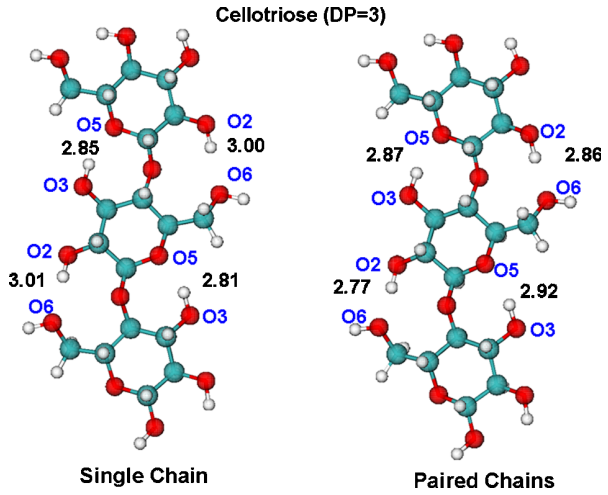

Figure 4. Compares the intra-chain hydrogen bond lengths in an isolated cellotriose chain and the corresponding paired chain.

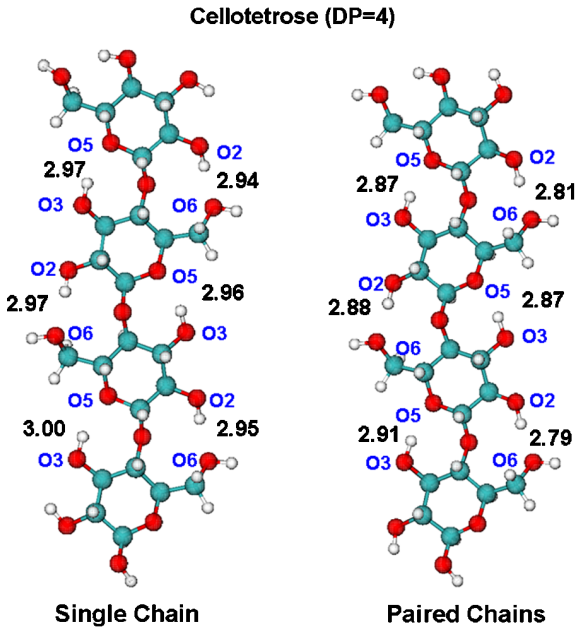

Figure 5. Compares the intra-chain hydrogen bond lengths in an isolated cellotetramer chain and the corresponding paired chain.

hydrogen bond length decreases from 2.92 Å to 2.86 Å upon alignment to form the inter-chain hydrogen bonds. The average bond angle also increases by about 2° upon pairing indicating an enhancement of the hydrogen bonding interaction. The same phenomenon is observed in cellotetramer as shown in Figure 5. The average hydrogen bond length is shortened by 0.09 Å from 2.95 Å in the isolated chain to 2.86 Å when the chains are aligned, whereas the average bond angle increases by about 3° exhibiting the enhancement of hydrogen bond strength. Tables 1–3 list the intra-chain hydrogen bond lengths for both the isolated and paired cellulose chains with DP values from 5 to 7. As shown, in all these cases, the intra-chain hydrogen bond lengths are shorter when the chains are aligned than those of the isolated chains indicating strong cooperative effect between the intra-chain and inter-chain hydrogen bonding interactions.

Table 1. Lists the intra-chain hydrogen bond lengths of O2H···O6 and O3H···O5 for isolated and paired cellulose chains with DP 5.

Single chain (DP = 5)		Paired chains (DP = 5)	
d (O2H···O6) (Å)	d (O3H···O5) (Å)	d (O2H···O6) (Å)	d (O3H···O5) (Å)
2.99	2.87	2.83	2.87
2.98	2.85	2.77	2.88
2.96	2.85	2.78	2.87
3.01	2.86	2.79	2.90

Table 2. lists the intra-chain hydrogen bond lengths of O2H···O6 and O3H···O5 for isolated and paired cellulose chains with DP 6.

Single chain (DP = 6)		Paired chains (DP = 6)	
d (O2H···O6) (Å)	d (O3H···O5) (Å)	d (O2H···O6) (Å)	d (O3H···O5) (Å)
2.94	2.94	2.79	2.84
2.88	2.99	2.76	2.84
2.76	3.06	2.73	2.80
2.87	2.96	2.78	2.82
2.98	2.96	2.80	2.87

Table 3. Lists the intra-chain hydrogen bond lengths of O2H···O6 and O3H···O5 for isolated and paired cellulose chains with DP 7.

Single Chain (DP = 7)		Paired Chains (DP = 7)	
d (O2H···O6) (Å)	d (O3H···O5) (Å)	d (O2H···O6) (Å)	d (O3H···O5) (Å)
2.98	2.93	2.83	2.88
2.99	2.92	2.77	2.88
2.99	2.91	2.76	2.84
2.98	2.89	2.78	2.85
2.96	2.90	2.80	2.89
3.01	2.91	2.78	2.93

The average bond angles increase by about 2–3° upon pairing which further confirms the cooperativity among intra-chain and inter-chain hydrogen bonds. This cooperative effect is very pronounced for all the cellulose chains studied from DP 2 to 7. In addition, even though each individual hydrogen bond may change its bond length slightly when more residues are added to the chain, there is no noticeable change in the average hydrogen bond lengths with different numbers of residues in the isolated chains. The average hydrogen bond angles also remain more or less the same when more residues are added to the chain. Similarly, the average intra-chain hydrogen bond lengths for the paired chains also remain more ore less the same at 2.86 Å with different number of residues. Again there is no noticeable change in average bond angles. This means that the cooperative effect is exhibited primarily between the inter-chain and intra-chain hydrogen bonding interaction, whereas there is little cooperative effect observed among the intra-chain hydrogen bonds. The mechanisms for this cooperative hydrogen bonding effect will be elucidated later in the section.

Besides intra-chain hydrogen bonding interactions, the inter-chain hydrogen bond interactions reveal very interesting phenomenon. Table 4 lists the inter-chain hydrogen bond lengths for cellulose chains with different number of glucose residues. Residue number one is the first glucose unit where the O6H group only acts as a proton donor, not as an acceptor. In all other residues, the O6H group is both a hydrogen bond donor and acceptor. From Table IV, it can be seen that only the inter-chain O6H···O3 hydrogen bond on residue one is significantly longer (~2.9 Å) than those of the other residues (~2.7 Å). This clearly shows the effect of cooperativity between the intra-chain and inter-chain hydrogen bonding interactions. On residue one, the O6H group is only a proton donor whereas the O3H group is only a proton acceptor. As a result, no enhancement of hydrogen bonding interaction is observed. The cooperativity effect is only pronounced when the O6H or O3H groups act as both proton donors and acceptors when the chains are aligned. There is no or very little cooperativity seen when the hydrogen bonds are isolated as in an unpaired cellulose chain where all the OH groups are either proton acceptors or donors, but not both.

We also carried out calculations to compare the hydrogen bond lengths and angles for an infinite cellulose chain, the infinite cellulose sheet and the bulk three dimensional cellulose structures. The hydrogen bonding parameters in both the origin and centre sheets in the bulk structure were determined and compared with the experimental values. Table 5 shows these parameters for both the intra-chain and inter-chain hydrogen bonds. For example, the intra-chain O2H···O6 hydrogen bond has a bond length of 2.96 Å and 3.00 Å in a single infinite chain. There is no obvious enhancement in hydrogen bond strength in an infinite chain. However, when the chains are aligned to form an infinite cellulose sheet, the O2H···O6 hydrogen bond lengths decrease to 2.76 Å and

Table 4. Lists the inter-chain O6H···O3 hydrogen bond lengths for cellulose chains with DP values varying from 1 to 7.

No. of glucose residue in a chain	Glucose residue 1 (Å)	Glucose residue 2 (Å)	Glucose residue 3 (Å)	Glucose residue 4 (Å)	Glucose residue 5 (Å)	Glucose residue 6 (Å)	Glucose residue 7 (Å)
7	2.90	2.71	2.71	2.72	2.71	2.69	2.71
6	2.91	2.69	2.71	2.70	2.72	2.72	
5	2.89	2.71	2.70	2.69	2.70		
4	2.89	2.71	2.71	2.71			
3	2.94	2.73	2.69				
2	2.88	2.69					
1	2.91						

Table 5. Compares the hydrogen bond lengths and angles of both the intra-chain O2H···O6 and O3H···O5 hydrogen bonds and the inter-chain O6H···O3 for the experimentally determined structures as well as theoretically determined one isolated infinite chain, an infinite sheet, and bulk structures.

	Origin sheet (exp.)	Centre sheet (exp.)	One chain (theo.)	One sheet (theo.)	Origin sheet (theo.)	Centre sheet (theo.)
d (O2H···O6) (Å)	2.76	2.86	2.96, 3.00	2.77, 2.79	2.76, 2.78	2.71, 2.72
d (O3H···O5) (Å)	2.76	2.70	2.79, 2.87	2.82, 2.84	2.72, 2.74	2.70, 2.71
d (O6H···O3) (Å)	2.89	2.71		2.77, 2.74	2.68 2.69	2.70, 2.72
∠ (O2H···O6)	150, 159	152, 165	171, 175	173, 170	171, 173	167, 170
∠ (O3H···O5)	137	162	149, 158	158, 163	162, 164	164, 164
∠ (O6H···O3)	144	157		162, 164	168, 168	166, 167

2.78 Å, respectively. These values are close to those in the bulk cellulose structures both calculated theoretically [8] and determined experimentally [7]. The same is observed for the bond angles and for the intra-chain O3H···O5 and inter-chain O6H···O3 hydrogen bonds. It clearly demonstrates that when the chains are paired to form the sheet, when the sheets are stacked to form the three dimensional structures, there is a strong enhancement, i.e. cooperativity, in the hydrogen bonding interactions.

Since the structures and the total energies for cellulose chains were determined at 0 K, the entropic effect was not taken into account in this study. However as temperature increases, entropy will play an increasingly important role in the structure and conformation of cellulose network. There will be more disorder in the hydrogen bonding structure at higher temperature. This effect was described in our earlier study [8] comparing theoretically determined hydrogen bonding network determined at 0K with experimentally determined crystalline cellulose Iβ structure at room temperature.

3.2 The mechanisms for hydrogen bonding cooperativity in celluloses

There are two models proposed in literature [11]–[13], [15], [16] to explain the mechanisms of hydrogen bonding cooperativity. One is based on electron delocalisation effect (charge transfer model) [11,12] while the other is based on electrostatic dipole interaction model [15,16]. Some earlier researchers further quantified the contributions of the charge transfer and electrostatic effects showing the dominant contribution of the former [13]. Figures 6 and 7 are the schematics of the charge transfer and electrostatic interaction models. In the charge transfer model, the hydrogen bonding interaction promotes electron transfer from the donor O in O6H group as in cellulose paired chains which acts as both proton donor and acceptor to the H in O2H group in the neighbouring residue of the same chain. This further polarises the O6H group which promotes additional electron transfer from the O in the O3H group in the adjacent chain to the H in O6H. Basically the inter-chain hydrogen bonding interaction enhances the intra-chain hydrogen bonding interaction, or vice versa. However, the O6H group has to be both a donor and acceptor in order for the mechanism to work. In native cellulose Iβ structure, both O6H and O3H groups are proton donors and acceptors. Clearly this mechanism applies to both these hydrogen bonding interactions. In the case of the first glucose residue in the paired cellulose chains, the O6H group is only a proton donor and O3H is acting only as a proton acceptor. As a result, the inter-chain hydrogen bond length on the first residue is significantly longer than those of the rest due to the lack of hydrogen bonding cooperativity. This charge transfer model shows that hydrogen bonding cooperativity is a short range phenomenon resulting from electron delocalisation or charge transfer. In the electrostatic model as shown in Figure 7, hydrogen bonding cooperativity originates from the dipole-dipole interactions between the hydrogen bonds. Since electrostatic Columbic interaction is a long range interaction and additive, it is a global effect. Obviously, the lack of substantial enhancement in hydrogen bonding interaction in the isolated cellulose chains in contrast to the paired cellulose chains show that electrostatic mechanism alone cannot explain the cooperativity in cellulose Iβ. The charge transfer mechanism is indeed the dominant mechanism for hydrogen bonding cooperativity observed in cellulose Iβ.

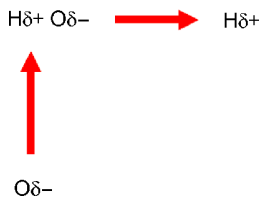

Figure 6. It is a schematic picture for the charge transfer (electron delocalisation) model to explain the cooperativity of hydrogen bonding interactions for the –OH group acting as both a proton donor and acceptor.

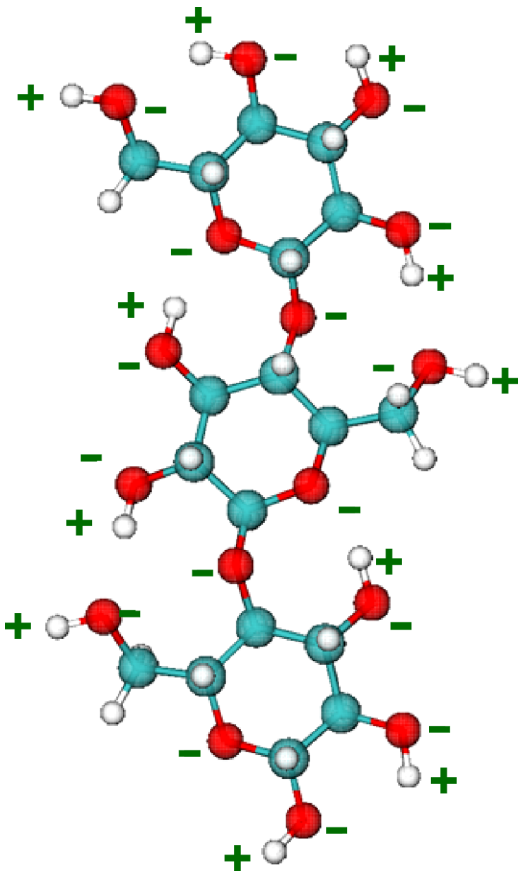

Figure 7. It is a schematic picture of the electrostatic interaction model for hydrogen bonding cooperativity.

3.3 The energetics of hydrogen bonding cooperativity in cellulose structures

Even though cooperativity among hydrogen bonds within an isolated chain is small, it is worthwhile to quantify its contribution, which is dominated by the electrostatic dipole interaction. This energy can then be compared with the cooperative energy between the inter-chain and intra-chain hydrogen bonds, which is dominated by the charge transfer effect. In order to determine quantitatively the effect of cooperativity on hydrogen bonding energy, the total energies of the isolated cellulose chains with residues varying from 1 to 7 were determined. The total energies of the corresponding paired cellulose chains were also determined.

Figure 8 shows the cumulative cooperative energies for both the isolated and paired cellulose chains with DP from 1 to 7. Even though the bond angles and lengths do not change very much in the isolated cellulose chains, there is some hydrogen bonding cooperativity due to electrostatic interaction. As expected, the electrostatic contribution to the total energy increases as more residues are added to the chain. The contribution to the 5 residue cellulose chain is about 5 kcal/mol (0.2 eV). This contribution increases

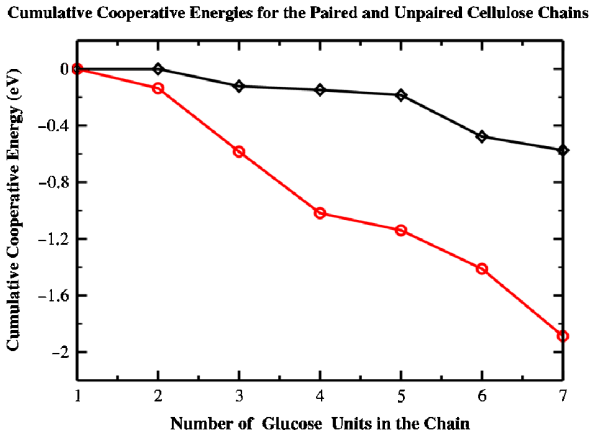

Figure 8. Shows the cumulative cooperative energies for the isolated and paired cellulose chains with DP from 1 to 7. The black diamond (◇) is for the isolated cellulose chains. The red circle (o) is for the paired cellulose chains.

to about 12.5 kcal/mol (0.5 eV) for cellulose chain with 6 residues and to about 15 kcal/mol (0.6 eV) for cellulose chain with 7 residues. The cumulative cooperative hydrogen bonding energy in paired cellulose chain is much larger than the corresponding isolated cellulose chain as can be seen from the figure. For example, the contribution of the cooperative effect to paired cellulose chain with 5 residues is about 28 kcal/mol (1.1 eV) compared to 5 kcal/mol. For DP 7, this contribution increases to about 48 kcal/mol (1.9 eV) compared to 15 kcal/mol for an isolated cellulose chain. It indeed confirms our previous conclusion from analysing the bond lengths and angles that charge transfer is the dominant contribution to the cooperative hydrogen bonding energy. The cooperative hydrogen energy is significant and may explain the recalcitrant nature of crystalline cellulose to chemical and enzymatic hydrolysis.

Figure 9 shows the non-cumulative total energy differences between the isolated and paired cellulose

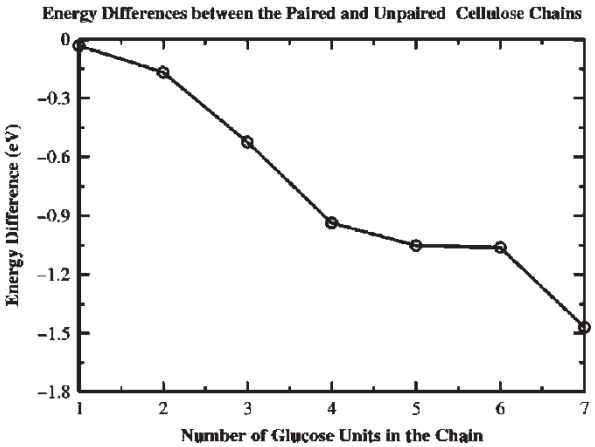

Figure 9. Shows the energy differences between the isolated and paired cellulose chains with DP varying from 1 to 7.

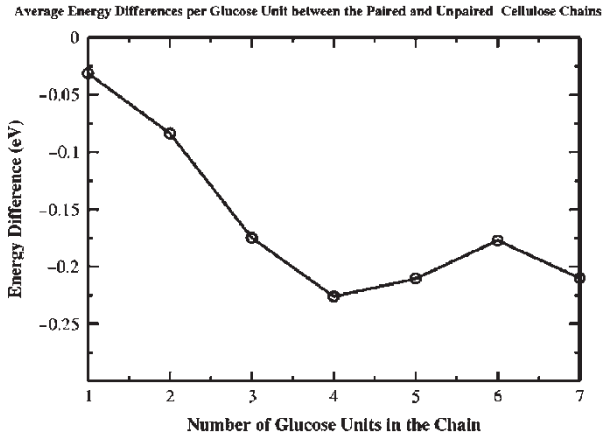

Figure 10. It is the average energy difference per glucose unit between the isolated and paired cellulose chains with DP = 1 to 7.

chains with different DP values. This energy difference comes from contribution of the inter-chain hydrogen bonding energy as well as cooperative effect due to alignment. Figure 10 shows the average energy change per glucose residue upon chain alignment to form inter-chain hydrogen bonds. It appears that the intra-chain and inter-chain hydrogen bonding cooperative effect increases dramatically from DP 1 to 4 then stabilises. This is mainly due to the edge effect. For the inter-chain hydrogen bond on residue 1 of the cellulose paired chains, there is no cooperative effect due to the lack of intra-chain and inter-chain coupling. For average cooperative energy per glucose unit, this effect would be more pronounced for small DP numbers ($1 \sim 4$) compared to the large DP values (>4).

4. Summary

A strong intra-chain and inter-chain hydrogen bonding cooperativity effect is observed in crystalline cellulose Iβ structures. This cooperativity is dominated by the charge transfer effect. It is present when the OH groups act as both a proton donor and acceptor in hydrogen bonding interactions. The electrostatic dipole interaction also affects the hydrogen bonding cooperativity, but the contribution is relatively small. The hydrogen cooperative effect could partially explain the recalcitrant nature of crystalline cellulose fibres to chemical and enzymatic hydrolysis. Besides as a raw material to produce biofuels, cellulose can be used in medical applications, as part of the composite materials or tissue engineering scaffold. This effect may be explored to engineer materials which have desired chemical, physical or mechanical properties.

Acknowledgements

Helpful discussions with Shi-You Ding and Mike Himmel from the National Renewable Energy Laboratory are gratefully acknowledged. Funding for this work comes from the start-up from Colorado State University (CSU). Some of the calculations were carried out at Engineering Computing Center at CSU.

References

[1] S.Y. Ding and M.E. Himmel, *The maize primary cell wall microfibril: a new model derived from direct visualization*, J. Agric. Food. Chem. 54 (2006), pp. 597–606.
[2] M.E. Himmel et al., *Biomass recalcitrance: engineering plants and enzymes for biofuels production*, Science 315 (2007), pp. 804–807.
[3] C. Somerville et al., *Toward a systems approach to understanding plant-cell walls*, Science 306 (2004), pp. 2206–2211.
[4] C. Somerville, *Cellulose synthesis in higher plants*, Annu. Rev. Cell. Dev. Biol. 22 (2006), pp. 53–78.
[5] R.H. Atalla and U.P. Agarwal, *Raman microprobe evidence for lignin orientation in the cell-walls of native woody tissue*, Science 227 (1985), pp. 636–638.
[6] Y. Nishiyama et al., *Crystal structure and hydrogen bonding system in cellulose 1(alpha), from synchrotron X-ray and neutron fibre diffraction*, J. Am. Chem. Soc. 125 (2003), pp. 14300–14306.
[7] Y. Nishiyama, P. Langan, and H. Chanzy, *Crystal structure and hydrogen-bonding system in cellulose 1 beta from synchrotron X-ray and neutron fibre diffraction*, J. Am. Chem. Soc. 124 (2002), pp. 9074–9082.
[8] X.H. Qian et al., *Atomic and electronic structures of molecular crystalline cellulose I beta: a first-principles investigation*, Macromolecules 38 (2005), pp. 10580–10589.
[9] A. Asensio, N. Kobko, and J.J. Dannenberg, *Cooperative hydrogen-bonding in adenine-thymine and guanine-cytosine base pairs. Density functional theory and Moller-Plesset molecular orbital study*, J. Phys. Chem. A 107 (2003), pp. 6441–6443.
[10] J. Ireta et al., *Density functional theory study of the cooperativity of hydrogen bonds in finite and infinite alpha-helices*, J. Phys. Chem. B 107 (2003), pp. 1432–1437.
[11] R. Wieczorek and J.J. Dannenberg, *Hydrogen-bond cooperativity, vibrational coupling, and dependence of helix stability on changes in amino acid sequence in small 3(10)-helical peptides. A density functional theory study*, J. Am. Chem. Soc. 125 (2003), pp. 14065–14071.
[12] R. Wieczorek and J.J. Dannenberg, *H-bonding cooperativity and energetics of alpha-helix formation of five 17-amino acid peptides*, J. Am. Chem. Soc. 125 (2003), pp. 8124–8129.
[13] A.V. Morozov, K. Tsemekhman, and D. Baker, *Electron density redistribution accounts for half the cooperativity of alpha helix formation*, J. Phys. Chem. B 110 (2006), pp. 4503–4505.
[14] K. Tsemekhman et al., *Cooperative hydrogen bonding in amyloid formation*, Protein Sci. 16 (2007), pp. 761–764.
[15] Y.D. Wu and Y.L. Zhao, *A theoretical study on the origin of cooperativity in the formation of 3(10)- and alpha-helices*, J. Am. Chem. Soc. 123 (2001), pp. 5313–5319.
[16] Y.L. Zhao and Y.D. Wu, *A theoretical study of beta-sheet models: Is the formation of hydrogen-bond networks cooperative?* J. Am. Chem. Soc. 124 (2002), pp. 1570–1571.
[17] N. Kobko and J.J. Dannenberg, *Cooperativity in amide hydrogen bonding chains. Relation between energy, position, and H-bond chain length in peptide and protein folding models*, J. Phys. Chem. A 107 (2003), pp. 10389–10395.
[18] B.F. King and F. Weinhold, *Structure and spectroscopy of $(HCN)_n$ clusters: cooperative and electronic delocalization effects in C-H...N hydrogen bonding*, J. Chem. Phys. 103 (1995), pp. 333–347.
[19] P. Carcabal et al., *Hydrogen bonding and cooperativity in isolated and hydrated sugars: mannose, galactose, glucose, and lactose*, J. Am. Chem. Soc. 127 (2005), pp. 11414–11425.
[20] L.L. Parker, A.R. Houk, and J.H. Jensen, *Cooperative hydrogen bonding effects are key determinants of backbone amide proton chemical shifts in proteins*, J. Am. Chem. Soc. 128 (2006), pp. 9863–9872.

[21] H.J. Song et al., *Cooperative effects and strengths of hydrogen bonds in open-chain cis-triaziridine clusters (*n = *2-8): A DFT investigation*, J. Phys. Chem. A 110 (2006), pp. 2225–2230.

[22] V. Horvath, Z. Varga, and A. Kovacs, *Long-range effects in oligopeptides. A theoretical study of the beta-sheet structure of Gly(n) (n = 2-10)*, J. Phys. Chem. A 108 (2004), pp. 6869–6873.

[23] M.J. Hardie et al., *Cooperative hydrogen bonding and yttrium(III) complexation in the assembly of molecular capsules*, Chem. Commun. (2000), pp. 849–850.

[24] S. Suhai, *Density functional theory of molecular solids: local versus periodic effects in the two-dimensional infinite hydrogen-bonded sheet of formamide*, J. Phys. Chem. 100 (1996), pp. 3950–3958.

[25] R. Ludwig, F. Weinhold, and T.C. Farrar, *Theoretical study of hydrogen bonding in liquid and gaseous* N-*methylformamide*, J. Chem. Phys. 107 (1997), pp. 499–507.

[26] R. Ludwig, F. Weinhold, and T.C. Farrar, *Structure of liquid* N-*methylacetamide: temperature dependence of NMR chemical shifts and quadrupole coupling constants*, J. Phys. Chem. A 101 (1997), pp. 8861–8870.

[27] CPMD3.11, http://www.cpmd.org, Copyrighted jointly by IBM Corp and by Max-Planck Institute, Stuttgart, 2007.

[28] W. Andreoni and A. Curioni, *New advances in chemistry and materials science with CPMD and parallel computing*, Parallel Computing 26 (2000), pp. 819–842.

[29] R. Car and M. Parrinello, *Unified approach for molecular-dynamics and density-functional theory*, Phys. Rev. Lett. 55 (1985), pp. 2471–2474.

[30] A.D. Becke, *Density-functional exchange-energy approximation with correct asymptotic-behavior*, Phys. Rev. A 38 (1988), pp. 3098–3100.

[31] C.T. Lee, W.T. Yang, and R.G. Parr, *Development of the Colle-Salvetti correlation-energy formula into a functional of the electron-density*, Phys. Rev. B 37 (1988), pp. 785–789.

[32] M. Sprik, J. Hutter, and M. Parrinello, *Ab initio molecular dynamics simulation of liquid water: comparison three gradient-corrected density functionals*, J. Chem. Phys. 105 (1996), pp. 1142–1152.

[33] C. Molteni and M. Parrinello, *Glucose in aqueous solution by first principles molecular dynamics*, J. Am. Chem. Soc. 120 (1998), pp. 2168–2171.

[34] N. Troullier and J.L. Martins, *Efficient pseudo-potentials for plane-wave calculations*, Phys. Rev. B 43 (1991), pp. 1993–2006.

[35] S.S. Xantheas, *Ab initio studies of cyclic water cluster* $(H_2O)_n$, *n = 1-6. III. Comparison of density functional with MP2 results*, J. Chem. Phys. 102 (1995), pp. 4505–4517.